Optica Applicata, Vol. LIV, No. 4, 2024
DOI: 10.37190/oa/192682

All-optical NOT and AND gates using nonlinear photonic crystal octagonal shape ring resonator

PRIYANKA KUMARI GUPTA[1,*], PUNYA PRASANNA PALTANI[1], SHRIVISHAL TRIPATHI[2]

[1]Department of Science and Mathematics, IIIT Naya Raipur, Chhattisgarh, India

[2]Department of ECE, IIIT Naya Raipur, Chhattisgarh, India

[*]Corresponding author: priyanka@iiitnr.edu.in

This paper proposes novel all-optical logic NOT and AND gates using an octagonal-shaped ring resonator with Kerr nonlinearity created on the platform of a two-dimensional photonic crystal (2DPC). The ring resonator offers maximum transmission efficiency and is simpler than the previously published designs. In our design, the nonlinearity is applied only to the outer rods of the core (rather than the whole core section) of the ring resonator, increasing their size. The proposed gates exhibit low operating and switching powers compared to the earlier proposals, which is highly desired for practically integrating any all-optical device.

Keywords: photonic crystals, all-optical logic gates, Kerr effect, FDTD.

1. Introduction

In recent years, the need and demand for high-speed data communication have increased rapidly, urging for devices that function entirely in the optical domain without the need for optical to electrical to optical (OEO) conversion [1]. In this context, all-optical devices using photonic crystals (PCs) have gained considerable attention and opened a new frontier among researchers because of their interesting characteristics and applicability in photonic integrated circuits (PICs). These periodic structures possess photonic bandgap (PBG), which can prohibit light propagation in specific frequency ranges [2,3]. Using PBG waveguides, optical devices with much smaller sizes and lower operating powers (compared to conventional waveguide devices) can be obtained. Numerous optical devices have been designed and explored for photonic integrated circuits thus far, such as all-optical switches [4], transistors [5], half subtractors [6], analog to digital converters [7], filters [8], multiplexers/demultiplexers [9], and so on.

In all-optical telecommunication networks and all-optical signal processing, various optical devices, mainly optical logic gates, play a critical role. Various mechanisms like waveguide interferometers [10], Mach–Zehnder interferometers [11], semiconduc-

tor optical amplifiers (SOAs) [12], resonant cavities [13], and directional couplers [14] have been used to propose all-optical logic gates employing linear and nonlinear PCs. However, complex integration, large size, and limited scope in performance are the major issues in the proposals mentioned above. All-optical logic gates designed using photonic crystal ring resonators (PCRRs) based on the Kerr nonlinear may provide effective performances in terms of efficient wavelength selection, easy implementation, and flexibility in design [15-17]. These PCRR structures consist of a resonant ring connecting the two waveguides, Bus and Drop. The resonant ring can filter and choose wavelengths in these configurations because optical waves can be directed to the Drop waveguide while passing through the bus waveguide at a particular resonant wavelength [18]. It is seen that the refractive index, radius, and core section dimensions of the resonant ring have a significant impact on the resonant wavelength of PCRR. When high-power optical waves are applied, the Kerr effect causes a change in the refractive index with light wave intensity in nonlinear dielectric materials. Thus, the optical behavior of the PCRR structure can be manipulated by varying the input intensity, and desired switching can be achieved [19].

Numerous structures for optical logic gates have been reported incorporating the Kerr effect based on photonic crystal ring resonators (PCRRs). However, in all these structures, the operating power intensity and the switching threshold power intensity are quite large, and the design of the core section of the resonant ring is also quite complex. For instance, ALIPOUR-BANAEI *et al*. (2014) [20] proposed a square ring resonator with a 12-fold quasi-crystal core section by removing a 7×7 array of dielectric rods in the core section of the resonant ring to design all-optical NOR and NAND gates using two nonlinear resonant rings. The operating and switching power intensity is 1 and 2 kW/μm^2, which is very large. Later, ALIPOUR-BANAEI *et al*. (2017) [21] proposed a 12-fold quasi-crystal core section identical to ALIPOUR-BANAEI *et al*. (2014) structure using a single resonant ring. The operating power intensity of 0.5 kW/μm^2 and switching threshold power intensity of 1.5 kW/μm^2 are used to design the NAND gate. However, using a single resonant ring could reduce the power intensity value. MEHDIZADEH *et al.* [22] proposed an all-optical NOR gate by using three square ring resonators with an octagonal core section. This proposed structure design is very large and complex as it uses three such resonant rings, which might not be suitable for photonic integration. The operating power intensity is 0.6 kW/μm^2, and the switching threshold power intensity is 1 kW/μm^2. In all these structures, the core section of these ring resonators involves changing the position of the rods manually, which increases the complexity and integration problem for large-scale circuits. Later, POURSALEH *et al*. reported an all-optical majority gate that operates at an operational power intensity of 1 kW/μm^2 and switching threshold power intensity of 2 kW/ μm^2 by cascading three 2-input OR gates using three square ring resonators. A good quality factor of 500 is achieved in their structures [23]. The resonator and core shape are identical in this case, but the device size is quite large. Hence, there is a need to design an appropriate ring resonator structure with a less complex core section that has nonlinear effects and can exhibit low oper-

ating and switching threshold power/intensities. Therefore, designing a simple ring resonator structure exhibiting lower operating and threshold power is the prime motive of the present paper. The inner part/section of our designed octagonal ring resonator maintains the device's symmetry and simplicity, allowing for a low-consumption, efficient device of reduced design complexity and high integration potential.

At the first step, an octagonal-shaped ring resonator structure with a nonlinear core created on 2D photonic crystals is proposed and discussed. The proposed structure differs from the conventional one in that only the outer rods of the core of the ring resonator are considered to be nonlinear with their slightly changed dimensions. The all -optical NOT and AND logic gate structures are proposed, using the designed ring resonator. Compared to the earlier works, the ring resonator structure proposed here is simple in design, exhibiting low operating and switching powers, which is highly desired for photonic integrated circuits. It is worth pointing out here that the optical inputs for both the proposed structures (NOT, AND) have the same wavelength and operating power intensity, showing compatibility and castability for their potential use in complex circuitry.

2. Photonic crystal octagonal shaped ring resonator (PCOSRR)

The fundamental structure consists of an array size of 31×35 dielectric circular rods positioned in the air. The dielectric rods are composed of chalcogenide glass having a refractive index value equal to 3.1 and a high nonlinear Kerr coefficient (n_2) equal to 9.1×10^{-17} m^2/W [24], making it suitable for optical switching. The radius of the dielectric rods (shown in purple color) is equal to $0.195 \times a$, where a is equal to 586 nm, the lattice constant of the structure. Further, two complete rows of dielectric rods along the X direction are removed to form waveguides, namely Bus and Drop. They are labeled as 'AB' and 'CD' with an octagonal shape ring resonator placed between them to design the structure. The octagonal shape ring resonator inner/core section is created using a 21×19 square array. Then, only the dielectric rods covering the outer core section of the resonant ring radius dimension are changed and are made nonlinear (shown in big brown color). A is the input port through which the light enters the structure. Ports B, C, and D are the output ports in this structure to analyze the output light. The diagram of the designed PCOSRR structure is shown in Fig. 1(a), respectively. The total footprint of the fundamental structure is about 372.48 μm^2.

The temporal and spatial step sizes must meet the following equation to achieve stable simulation.

$$c\,\Delta t \le \left(\frac{1}{\Delta x^2} + \frac{1}{\Delta z^2} \right)^{-1/2} \tag{1}$$

where c is the free-space velocity of light, Δt is the time interval, and Δx and Δz are the intervals between two neighboring grid points along the x and z axis ($\Delta x = \Delta z =$

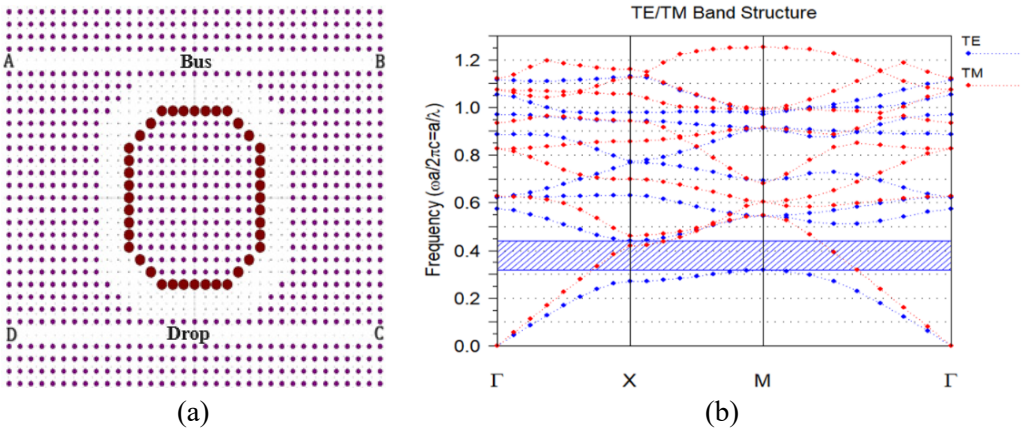

(a) (b)

Fig. 1. (a) The fundamental structure and (b) the dispersion diagram of the proposed structure in TE mode with PBG range.

= $a/16$). The perfectly matched layer (PML) absorbing boundary conditions are used to reduce reflection loss from the boundary, and its width is chosen as 5 μm. The dispersion/bandgap diagram of the proposed PCOSRR structure for TE/TM mode is obtained and calculated by using the plane wave expansion (PWE) method [25], as shown in Fig. 1(b). A bandgap region is obtained in the normalized frequency range (a/λ) between 0.316 to 0.441 for TE mode only, corresponding to the wavelength range between 1331 nm to 1890 nm covering the telecommunication window. Hence, this region is chosen for proposing the logic gates.

The resonant wavelength of the resonant rings depends on the refractive index of the dielectric rods present in the resonant ring core, which in turn depends on the power intensity of the incident optical wave due to the Kerr effect. Therefore, the optical behavior of the nonlinear resonant ring can be controlled by applying high-power optical intensity. In our proposed structure, the refractive index of the dielectric rods covering the core is thus changed by applying the nonlinear optical Kerr effect. The refractive index change obtained by applying optical power intensity is given by

$$n = n_0 + \Delta n \tag{2}$$

Here, n_0 is the linear refractive index, and Δn is the change in the refractive index of the nonlinear material induced by the electric field of the incident light and can be written as [26]

$$\Delta n = n_2 I \tag{3}$$

Where n_2 is the Kerr coefficient of the nonlinear material, and I is the optical power intensity of the input light. The intensity of the launch beam is proportional to $|E|^2$,

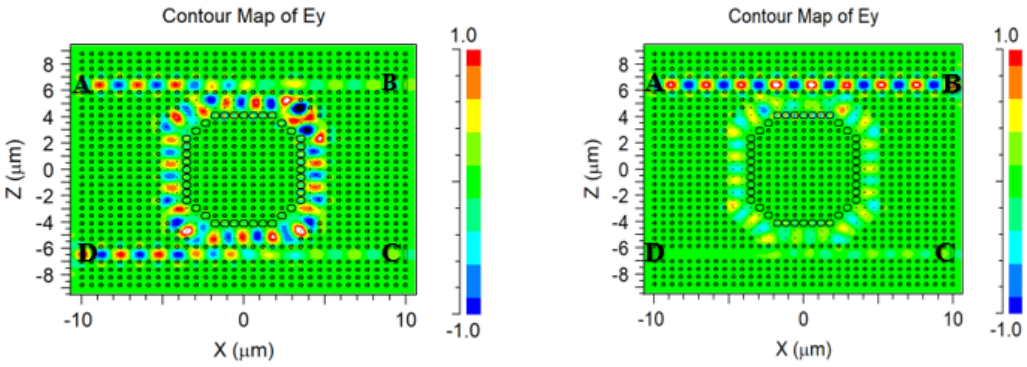

(a) (b)

Fig. 2. The low and high input intensity optical wave distribution of the proposed nonlinear octagonal shape photonic crystal ring resonator at (a) 0.373 kW/μm^2 and (b) 0.690 kW/μm^2.

where E is the electric field distribution of the incident light. Third-order nonlinear susceptibility (χ^3) is related to the Kerr coefficient n_2, which is given by

$$\chi^3 = \frac{4 n_0^2 n_2}{3 Z_0} \tag{4}$$

where Z_0 is the impedance of free space.

The optical behavior or the electric field distribution of the proposed structure is shown in Fig. 2. In the proposed design, when a low input power intensity (I = = 0.373 kW/μm^2) is applied, the change in the refractive index (Δn) of the nonlinear ring rods in the core section equals 0.0336. Thus, the input power transmits to the port D entirely due to the resonance effect and works in the linear region, and the dropping task occurs, as shown in Fig. 2(a). But when high input power intensity (I = 0.690 kW/μm^2), the output light transmits to port B entirely due to the Kerr effect, as shown in Fig. 2(b). The change in the refractive index of the nonlinear ring rods is found to be Δn = 0.0621. So, at high input power intensity, the output switches completely from port D to port B, respectively. Thus, the switching threshold mechanism is for the proposed structure. When the input power intensity exceeds the switching threshold power near the resonant ring, the dropping task is not performed. So, we can conclude that the low power input intensity (P_o = 0.373 kW/μm^2) is the operational optical intensity, and the high input power intensity (P_t = 0.690 kW/μm^2) is the switching threshold optical intensity obtained for this structure.

The output spectrum for the proposed structure for low input power intensity (P_o = = 0.373 kW/μm^2) is shown in Fig. 3. From this, the resonant wavelength is found at λ = 1552 nm. Furthermore, the coupling and dropping efficiencies are 100% for our proposed structure, with a quality factor Q equal to 970. The quality factor Q is deter-

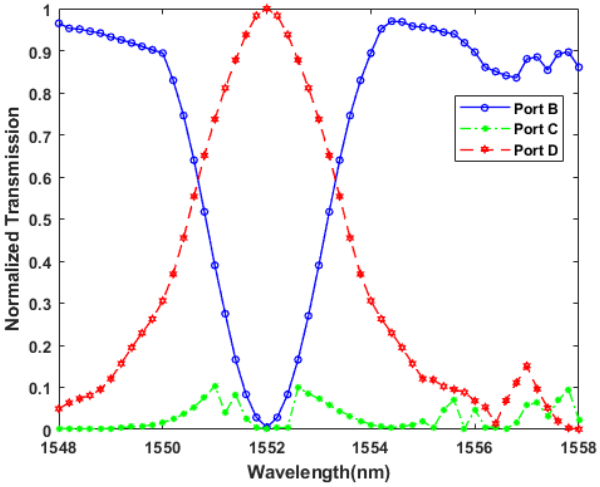

Fig. 3. The proposed structure's normalized output spectrum for low input power intensity (0.373 kW/μm^2).

mined as the ratio of resonant wavelength λ_0 and spectral width $\Delta\lambda$. The simulation is done using the two-dimensional FDTD method [27]. The proposed structure behaves as an intensity-dependent optical switch. So, the proposed structure can be considered for designing the optical logic gates. Extending the idea further, NOT and AND logic gates are proposed in the subsequent section.

3. All-optical NOT gate

3.1. Design configuration

To realize the NOT gate, the fundamental structure is slightly modified with the ring resonator placed vertically downward by increasing the rods in both directions. Now,

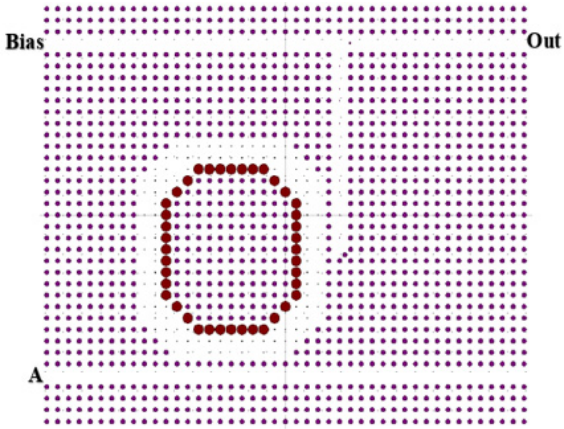

Fig. 4. The proposed NOT gate has one input port A, one bias port (Bias), and one output port (Out).

T a b l e 1. The working state of the proposed NOT gate structure.

Bias	A	Logic output NOT	Transmission T $\lvert E_0/E_{in}\rvert^2$
1	0	1	≥ 0.5
1	1	0	< 0.2

the structure consists of a nonlinear PCRR surrounded by three waveguides. The first two waveguides are created by removing two complete rows of rods along the X direction. The first waveguide corners are marked as Bias and Out. The second waveguide is marked as A. Then, a third waveguide is formed by removing a few rods along the Z direction, which connects the ring resonator through the first waveguide. The final proposed NOT gate structure consists of one input port (A), one bias port (Bias,) and one output port (Out), as shown in Fig. 4. The working states of the proposed NOT logic gate are shown in Table 1. The logical '1' transmission is determined by a value of 0.5 or greater, and logical '0' by a value less than 0.2, as indicated in Table 1.

3.2. Simulation results

For simulation, the power intensity values are kept equal to $P_o = 0.373$ kW/μm^2 for the bias and the input ports. Also, the operating wavelength for the bias and input ports are kept the same, equal to 1552 nm. Hence, the same wavelength (1552 nm) and power intensities (0.373 kW/μm^2) are applied to the input ports 'Bias' and 'A'. This makes the device cascadeable. Further, the bias port is kept ON (Bias = 1) for the NOT gate. When the input port is OFF (A = 0), the optical power intensity from both ports towards the resonator is 0.373 kW/μm^2. According to the theory, the light should couple into the resonator. However, because of a third waveguide connected to the ring resonator, the light from the bias port does not couple into the resonator. Therefore, the light trav-

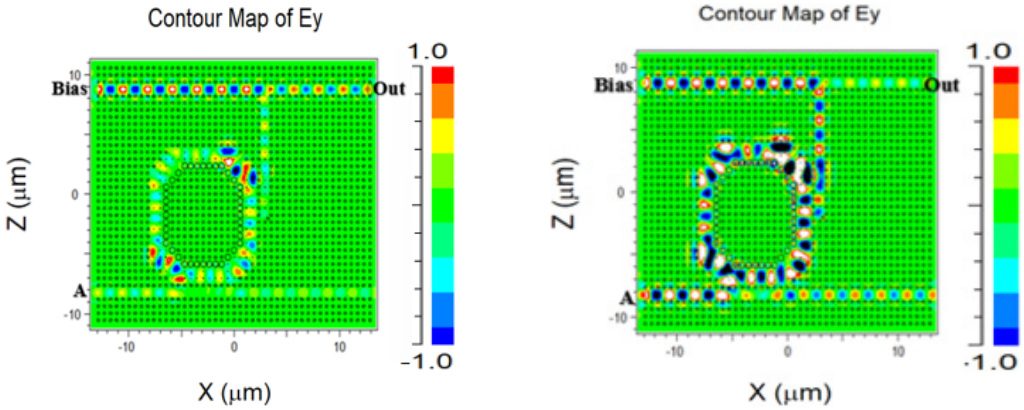

Fig. 5. The snapshot of the proposed NOT gate structure's different states shows input port A's logic conditions.

T a b l e 2. The truth table of the proposed NOT gate structure.

Bias port 'Bias'		Input port 'A'		Output port 'Out' (NOT gate)	
Logic level	Corresponding power	Logic level	Corresponding power	Logic level	Transmitted power
1	P_o	0	0	1	0.61
1	P_o	1	P_o	0	0.16

els straight to the output port 'Out'. The output port 'Out' will become ON (Out = 1), as shown in Fig. 5(a).

For the second case, the input port 'A' is ON (A = 1), and the total combined optical power intensity due to the bias and input becomes 0.746 kW/μm^2. So, when the light travels from the bias and input towards the ring resonator, strong light coupling occurs in the resonant ring, due to which the output travels to the output port (Out) with a minimal output efficiency. So, the port 'Out' will be OFF (Out = 0), as shown in Fig. 5(b). The results show that the gate acts as a 'NOT' gate. The truth table of the proposed NOT gate structure is shown in Table 2.

4. All-optical AND gate

4.1. Design configuration

For the AND logic gate, a Y-shaped junction is created, which serves as the input waveguide. The intersection consists of two waveguides, denoted by A1 and A2. Previously, a Gaussian pulse was launched at port A, but now two input ports, A1 and A2, are considered through which the light is launched. A third waveguide is then used to connect the ring resonator to the output port B. The output ports C and D are set similarly to the fundamental structure to observe the light coming through them, as shown in Fig. 6.

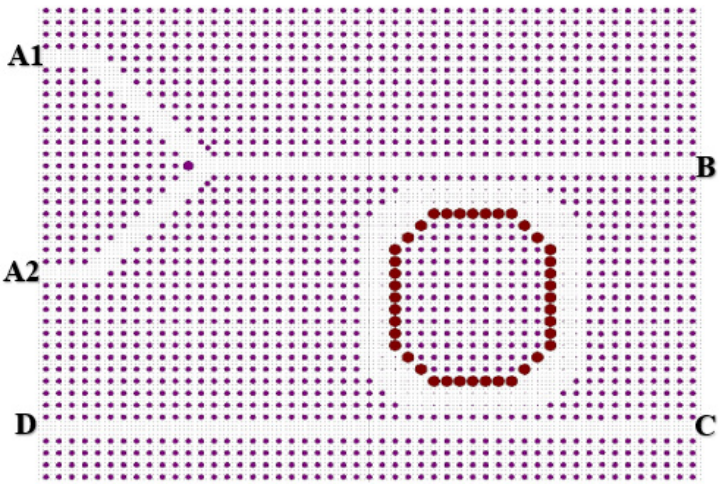

Fig. 6. The proposed AND gate has two input ports, A1 and A2, and the B output port.

T a b l e 3. The working state of the proposed AND gate structure.

Port A1	Port A2	Logic output AND	Transmission T $\lvert E_0/E_{in}\rvert^2$
0	0	0	0
0	1	0	< 0.2
1	0	0	< 0.2
1	1	1	≥ 0.5

This feature of using identical wavelengths and power intensities in the inputs makes the device compatible and cascadable. Also, it is essential to mention that both the input ports are isolated. The working states of the proposed AND logic gate are shown in Table 3. The logical '1' transmission is determined by a value of 0.5 or greater, and logical '0' by a value less than 0.2, as indicated in Table 3.

4.2. Simulation results

For simulation, a Gaussian light pulse is launched at two input ports, A1 and A2, with an operating wavelength of 1552 nm and power intensity of 0.373 kW/μm^2. The struc-

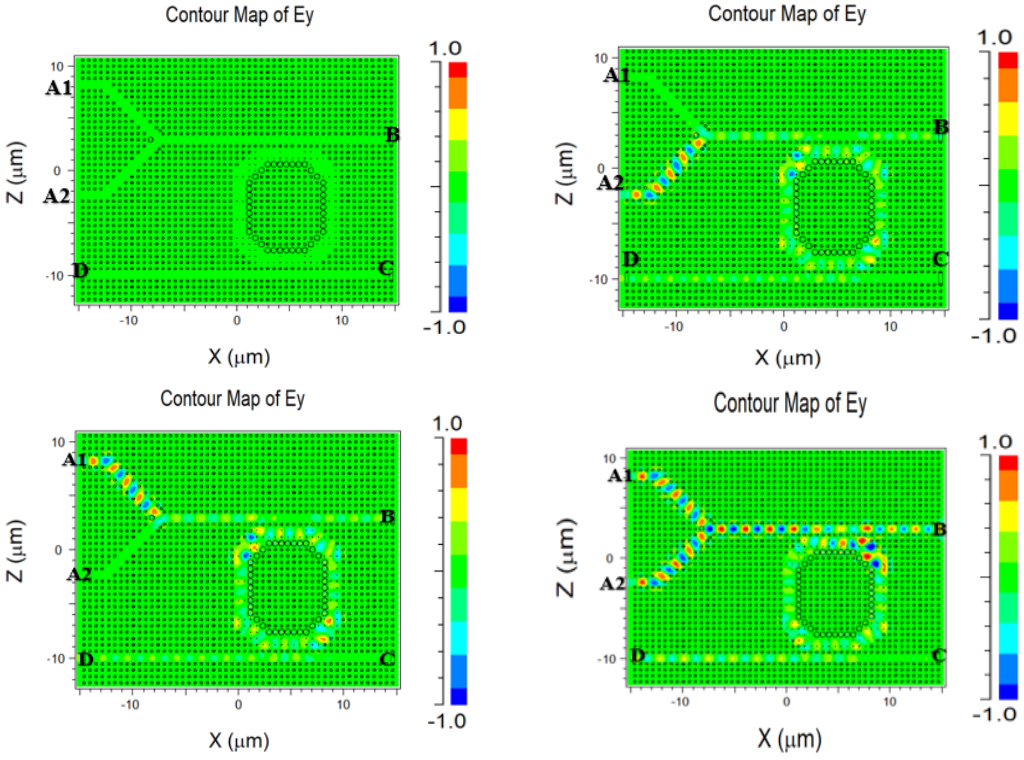

Fig. 7. The snapshot of the different states of the proposed AND gate structure for different logic conditions of input ports A1 and A2.

tures are simulated, and snapshots of the AND gate for different logic conditions of A1 and A2 for the designed structure are shown in Fig. 7. When both inputs ports A1 and A2 are OFF (A1 = A2 = 0), the input intensity is zero (0 kW/μm^2). Hence, the output at ports B, C, and D is zero (0 kW/μm^2), and all the output ports are OFF, as shown in Fig. 7(a). In the case when A1 is OFF and A2 is ON (A1 = 0, A2 = 1), the optical power coming from A2 will be able to travel toward the PCRR with an optical power intensity of 0.373 kW/μm^2, so according to the theory, the output light should travel towards port D. The resonant wavelength gets detuned/decoupled with the input power intensity due to the Y-junction in front of the ring resonator. As a result, the light travels with a very low output efficiency through the resonant ring. So, the obtained output at port D is of very low power (or efficiency). Also, the output obtained at ports B and C is subsequently low, as shown in Fig. 7(b).

A similar simulation result is observed when A1 = ON and A2 is OFF (A1 = 1, A2 = 0), as shown in Fig. 7(c). In this case, the output power value is low for ports B, C, and D. But when both the input ports A1 and A2 are ON (A1 = 1, A2 = 1), the optical input light intensity (0.373 kW/μm^2) from both ports travels towards the ring resonator. In this case, the collective power intensities from both input ports equal 0.746 kW/μm^2. So, as the total intensity exceeds the threshold, the light gets detuned/decoupled from

T a b l e 4. The truth table of the proposed AND gate structure.

Input port A1		Input port A2		Output port B (AND gate)	
Logic level	Corresponding power	Logic level	Corresponding power	Logic level	Transmitted power
0	0	0	0	0	0.00
0	0	1	P_o	0	0.15
1	P_o	0	0	0	0.19
1	P_o	1	P_o	1	0.96

T a b l e 5. Comparison of related works and the proposed work mentioned in the literature.

Related work	Resonator shape	Operating wavelength [nm]	Operating power intensity [kW/μm^2]	Switching threshold power intensity [kW/μm^2]	Proposed logic gates
[20]	Square + circular core section	1550	1	2	NOR NAND
[21]	Square + circular core section	1554	0.50	1.50	NAND
[22]	Square + octagonal core section	1550	0.60	1	NOR
[23]	Square + square core section	1550	1	2	OR
Proposed work	Octagonal + octagonal core section	1552	0.373	0.690	NOT AND

the ring resonator and travels straight to port B. Hence, the output light is at port B, as shown in Fig. 7(d). Therefore, we can conclude that port B acts as an AND gate. The truth table of the proposed AND gate structure is shown in Table 4.

Table 5 contains information about the resonator shape, operating power intensity, switching threshold power intensity, proposed logic gates of the proposed structure, and related works available in the literature for reference. It is worth noting that the operating powers and switching threshold powers obtained are significantly lower when a large Kerr coefficient is used. The input ports used in the structure have the same operating power intensity and same wavelength value, which makes the device cascadebility.

5. Conclusion

An octagonal-shaped ring resonator structure with a nonlinear core created on 2D photonic crystals is designed to propose the all-optical NOT and AND logic gates. The structure exhibits coupling and dropping efficiencies of 100%. The resonance wavelength of the ring resonator is found to be 1552 nm. The operating power (0.373 kW/μm^2) is the same for both logic gates which makes them cascadable. The gates exhibit a switching power of 0.690 kW/μm^2. The PWE and FDTD methods are used to simulate and analyze the proposed structure. Low operating and switching powers allow the implementation of the proposed gates in photonic integrated devices/circuits.

References

[1] Sakoda K., *Optical Properties of Photonic Crystals*, Springer Science & Business Media, 2001.

[2] Kalra Y., Sinha R.K., *Modelling and design of complete photonic band gaps in two-dimensional photonic crystals*, Pramana **70**(1), 2008: 153-161. https://doi.org/10.1007/s12043-008-0013-4

[3] Meade R.D., Brommer K.D., Rappe A.M., Joannopoulos J.D., *Existence of a photonic band gap in two dimensions*, Applied Physics Letters **61**(4), 1992: 495-497. https://doi.org/10.1063/1.107868

[4] Gupta P.K., Paltani P.P., Tripathi S., *Photonic crystal based all-optical switch using a ring resonator and Kerr effect*, Fiber and Integrated Optics **41**(5-6), 2022: 143-153. https://doi.org/10.1080/01468030.2022.2163725

[5] Medhekar S., Paltani P.P., *All-optical passive transistor using counter-propagating beams in a nonlinear Mach-Zehnder interferometer*, Fiber and Integrated Optics **28**(4), 2009: 268-274. https://doi.org/10.1080/01468030902759307

[6] Parandin F., Malmir M.-R., Naseri M., *All-optical half-subtractor with low-time delay based on two-dimensional photonic crystals*, Superlattices and Microstructures **109**, 2017: 437-441. https://doi.org/10.1016/j.spmi.2017.05.030

[7] Shamsi A., Moradi R., *All optical analog to digital convertor using nonlinear photonic crystal ring resonators*, Optical and Quantum Electronics **52**(10), 2020: 435. https://doi.org/10.1007/s11082-020-02541-z

[8] Gupta P.K., Tripathi S., Paltani P.P., *Optical add/drop filter and pressure sensor design using two-dimensional photonic crystal*, 2022 Workshop on Recent Advances in Photonics (WRAP), Mumbai, India, IEEE, 2022: 1-2. https://doi.org/10.1109/WRAP54064.2022.9758383

[9] Tavousi A., *Wavelength-division demultiplexer based on hetero-structure octagonal-shape photonic crystal ring resonators*, Optik **179**, 2019: 1169-1179. https://doi.org/10.1016/j.ijleo.2018.10.125

[10] HUSSEIN H.M.E., ALI T.A., RAFAT N.H., *A review on the techniques for building all-optical photonic crystal logic gates*, Optics & Laser Technology **106**, 2018: 385-397. https://doi.org/10.1016/j.optlastec.2018.04.018
[11] GUPTA M.M., MEDHEKAR S., *All-optical NOT and AND gates using counter propagating beams in nonlinear Mach–Zehnder interferometer made of photonic crystal waveguides*, Optik **127**(3), 2016: 1221-1228. https://doi.org/10.1016/j.ijleo.2015.10.176
[12] LI Z., LIU Y., ZHANG S., JU H., DE WAARDT H., KHOE G.D., DORREN H.J.S., LENSTRA D., *All-optical logic gates using semiconductor optical amplifier assisted by the optical filter*, Electronics Letters **41**(25), 2005. https://doi.org/10.1049/el:20053385
[13] GUPTA P.K., PALTANI P.P., TRIPATHI S., *All-optical simultaneous OR and NAND gates using photonic crystal ring resonator and Kerr effect*, Physica Scripta **99**, 2024: 015021. https://doi.org/10.1088/1402-4896/ad1651
[14] SHARIFI H., HAMIDI S.M., NAVI K., *All-optical photonic crystal logic gates using nonlinear directional coupler*, Photonics and Nanostructures - Fundamentals and Applications **27**, 2017: 55-63. https://doi.org/10.1016/j.photonics.2017.10.002
[15] VEISI E., SEIFOURI M., OLYAEE S., *A novel design of all-optical high speed and ultra-compact photonic crystal AND logic gate based on the Kerr effect*, Applied Physics B **127**, 2021: 70. https://doi.org/10.1007/s00340-021-07618-5
[16] RAHMANI A., ASGHARI M., *An ultra-compact and high speed all-optical OR/NOR gate based on nonlinear PhCRR*, Optik **138**, 2017: 314-319. https://doi.org/10.1016/j.ijleo.2017.03.034
[17] SALMANPOUR A., MOHAMMADNEJAD S., BAHRAMI A., *All-optical photonic crystal AND, XOR, and OR logic gates using nonlinear Kerr effect and ring resonators*, Journal of Modern Optics **62**(9), 2015: 693-700. https://doi.org/10.1080/09500340.2014.1003256
[18] REBHI S., NAJJAR M., *A new design of a photonic crystal ring resonator based on Kerr effect for all-optical logic gates*, Optical and Quantum Electronics **50**(10), 2018: 358. https://doi.org/10.1007/s11082-018-1628-4
[19] SALMANPOUR A., MOHAMMADNEJAD S., OMRAN P.T., *All-optical photonic crystal NOT and OR logic gates using nonlinear Kerr effect and ring resonators*, Optical and Quantum Electronics **47**(12), 2015: 3689-3703. https://doi.org/10.1007/s11082-015-0238-7
[20] ALIPOUR-BANAEI H., SERAJMOHAMMADI S., MEHDIZADEH F., *All-optical NOR and NAND gate based on nonlinear photonic crystal ring resonators*, Optik **125**(19), 2014: 5701-5704. https://doi.org/10.1016/j.ijleo.2014.06.013
[21] ALIPOUR-BANAEI H., SERAJMOHAMMADI S., MEHDIZADEH F., *All-optical NAND gate based on nonlinear photonic crystal ring resonators*, Optik **130**, 2017: 1214-1221. https://doi.org/10.1016/j.ijleo.2016.11.190
[22] MEHDIZADEH F., SOROOSH M., *Designing of all-optical NOR gate based on photonic crystal*, Indian Journal of Pure & Applied Physics **54**, 2016: 35-39.
[23] POURSALEH A., ANDALIB A., *An all-optical majority gate using nonlinear photonic crystal based ring resonators*, Optica Applicata **49**(3), 2019: 487-498. https://doi.org/10.5277/oa190310
[24] OGUSU K., YAMASAKI J., MAEDA S., KITAO M., MINAKATA M., *Linear and nonlinear optical properties of Ag–As–Se chalcogenide glasses for all-optical switching*, Optics Letters **29**(3), 2004: 265-267. https://doi.org/10.1364/OL.29.000265
[25] JOHNSON S.G., JOANNOPOULOS J.D., *Block-iterative frequency-domain methods for Maxwell's equations in a planewave basis*, Optic Express **8**(3), 2001: 173-190. https://doi.org/10.1364/OE.8.000173
[26] OKAMOTO K., *Fundamentals of Optical Waveguides*, Elsevier, 2021.
[27] TAFLOVE A., *Computational Electrodynamics: The Finite-difference Time-domain Method*, Artech House, 1995.

Received April 5, 2024
in revised form July 25, 2024